

# A Bayesian joint model of multiple longitudinal and categorical outcomes with application to multiple myeloma using permutation-based variable importance

Danilo Alvares<sup>1,\*</sup>, Jessica K. Barrett<sup>1</sup>, François Mercier<sup>2</sup>, Jochen Schulze<sup>2</sup>,  
Sean Yiu<sup>3</sup>, Felipe Castro<sup>2</sup>, Spyros Roumpanis<sup>2</sup>, and Yajing Zhu<sup>2,\*\*</sup>

<sup>1</sup>MRC Biostatistics Unit, University of Cambridge, U.K.

<sup>2</sup>F. Hoffmann-La Roche Ltd, Basel, Switzerland

<sup>3</sup>Roche Products Ltd, Welwyn Garden City, U.K.

\**email:* danilo.alvares@mrc-bsu.cam.ac.uk

\*\**email:* yajing.zhu@roche.com

## Abstract

Joint models have proven to be an effective approach for uncovering potentially hidden connections between various types of outcomes, mainly continuous, time-to-event, and binary. Typically, longitudinal continuous outcomes are characterized by linear mixed-effects models, survival outcomes are described by proportional hazards models, and the link between outcomes are captured by shared random effects. Other modeling variations include generalized linear mixed-effects models for longitudinal data and logistic regression when a binary outcome is present, rather than time until an event of interest. However, in a clinical research setting, one might be interested in modeling the physician’s chosen treatment based on the patient’s medical history to identify prognostic factors. In this situation, there are often multiple treatment options, requiring the use of a multiclass classification approach. Inspired by this context, we develop a Bayesian joint model for longitudinal and categorical data. In particular, our motivation comes from a multiple myeloma study, in which biomarkers display nonlinear trajectories that are well captured through bi-exponential submodels, where patient-level information is shared with the categorical submodel. We also present a variable importance strategy to rank prognostic factors. We apply our proposal and a competing model to the multiple myeloma data, compare the variable importance and inferential results for both models, and illustrate patient-level interpretations using our joint model.

**Keywords:** Bayesian inference; Bi-exponential model; Categorical data; Model-agnostic; M-protein dynamics.

# 1 Introduction

In recent years, there has been a growing interest in joint models that simultaneously analyze longitudinal and time-to-event outcomes (Ibrahim et al., 2010; Alsefiri et al., 2020). A standard joint model comprises a single longitudinal outcome characterized by a linear mixed-effects submodel, a single survival outcome described by a proportional hazards submodel, and an association structure that connects both submodels (Rizopoulos, 2012). In most cases, this connection involves random effects and complex integrals associated with the survival function, but the current literature also presents other alternatives, such as latent classes that stratify heterogeneous subpopulations (Proust-Lima et al., 2014; Andrinopoulou et al., 2020), marginal submodels connected by a copula (Ganjali and Baghfalaki, 2015; Cho et al., 2024), and separate random effects without the need to perform numerical integration (Alvares and Rubio, 2021).

Many authors have extended the standard joint model. For example, some studies modeled multiple longitudinal outcomes and/or competing risks (Hickey et al., 2016; Rué et al., 2017; Rustand et al., 2024), while others incorporated the dependence of spatial random effects into the joint modeling (Martins et al., 2016, 2017; Rappl et al., 2023). There were also proposals that considered categorical longitudinal and survival outcomes (Choi et al., 2015; Chi et al., 2024), two longitudinal submodels, one continuous and one ordinal (Delporte et al., 2024), and joint models of longitudinal continuous and binary data (Wang et al., 2000; Horrocks and van Den Heuvel, 2009; Lu et al., 2016; Zhou et al., 2023). For the latter, to the best of our knowledge, there are currently no extensions available that accommodate more than two categories. This extension introduces at least two additional complexities: (i) more parameters to be estimated, which requires more data, and (ii) imbalanced categories, leading to poor predictive performance (Kolo, 2010).

To fill this gap in the literature, we developed a Bayesian joint model for longitudinal and categorical outcomes. Our proposal is motivated by a retrospective cohort study from a real-world database of patients diagnosed with multiple myeloma in the United States between January 2015 and February 2022. In this application, there are two nonlinear longitudinal biomarkers that are modeled through bi-exponential submodels (Claret et al., 2009; Thai et al., 2022). The bi-exponential model includes three components (baseline, growth rate, and decay rate) that summarize the temporal dynamics of each biomarker and potentially help to explain the physician’s chosen treatment. Furthermore, we considered three treatment options that can be described using a (nominal) categorical submodel (Agresti, 2013). The longitudinal and categorical submodels are connected by sharing the patient-level baseline, growth rate, and decay rate parameters. The main research question here is what are the key factors supporting the physician’s chosen treatment. This is motivated by the clinical knowledge that there is a set of factors contributing to treatment choice, but very rarely are there quantifications of the relative contribution of each of them.

The adequacy of the bi-exponential submodels is verified through an analysis of individual weighted residuals (Desmée et al., 2017), while performance of the categorical submodel is evaluated using metrics for multiclass classification (Grandini et al., 2020). Moreover, as a complement to posterior inference, we present a model-agnostic variable importance approach with the aim of improving the transparency, trustability, and

interpretability of the results (Casalicchio et al., 2019).

The outline of the work is as follows. Section 2 presents the multiple myeloma retrospective cohort study that serves as the foundation for the Bayesian joint model of multiple longitudinal and categorical outcomes, introduced in Section 3. Section 4 discusses a variable importance strategy for the proposed joint model. In Section 5, we apply our joint model and a competing model to the multiple myeloma data, compare classification metrics, variable importance, and inferential results between both models, and illustrate patient-level interpretations using our proposal. Finally, in Section 6, concluding remarks are provided.

## 2 Multiple myeloma data

Multiple myeloma (MM) is a type of blood cancer that affects plasma cells. These cancerous plasma cells multiply uncontrollably, eventually crowding out healthy blood cells in the bone marrow, and secrete a monoclonal protein/paraprotein, also known as M-protein (van de Donk et al., 2021). The main MM symptoms are bone pain, weakness, fatigue, frequent infections, and easily broken bones, as well as potentially causing kidney and immune system problems (Kumar et al., 2017). MM treatments may include targeted therapy, e.g. proteasome inhibitors and immunomodulatory agents, chemotherapy, stem cell transplant, and immune-based therapies including T-cell engaging antibodies and CAR-T (Rajkumar and Kumar, 2020). While there is currently no cure for MM, the advent of new treatments has led to an increase of progression free survival and overall survival (Gulla and Anderson, 2020).

### 2.1 Data source and eligibility criteria

For illustrating our joint model proposal, we used a Flatiron Health electronic health record (EHR)-derived de-identified database of patients who were diagnosed with MM in the US between 1st January 2015 and 28th February 2022 (Birnbaum et al., 2020; Ma et al., 2023). During the study period, the de-identified data came from over 280 US cancer clinics (approximately 800 sites of care). The majority of patients in the database originate from community oncology settings; relative community/academic proportions may vary depending on study cohort. Other eligibility criteria are: (i) at least 18 years of age at MM diagnosis, (ii) no longer than 60 days between initial diagnosis and first activity (visit or line of therapy initiation), (iii) more than three months on-treatment before the end of study follow-up, (iv) no malignancies before MM diagnosis, and (v) patients treated with RVd (a three-drug therapy composed of Lenalidomide, Bortezomib, and Dexamethasone) in the first line of therapy, which was oncologist-defined and rule-based, and is one of the most common regimens for patients with newly diagnosed MM (Punke et al., 2017). The last criterion ensures the homogeneity of the selected subpopulation with respect to the initial treatment received. Thus, 1579 patients met all eligibility criteria.

## 2.2 Outcomes and baseline covariates

Since all selected patients are initially treated with RVd, we are interested in studying what are the key factors contributing to a physician’s chosen treatment for the second line of therapy. Hence, the primary outcome in this study is the treatment assigned to the patient after RVd, in which we considered three options: (I) Carfilzomib-based therapy, (II) Pomalidomide-based therapy, or (III) other therapy. Carfilzomib-based and Pomalidomide-based therapies were chosen because they are the most frequently used treatments. Other therapy add up to 121 regimens, including treatments that combine Carfilzomib plus Pomalidomide (7%). Supplementary Appendix A shows the 15 most frequent regimens that make up the other therapy. We also have secondary outcomes, which are longitudinal biomarkers –M-spike and serum free light chains (FLC)– that measure the concentration of M-protein and the involved light chain in serum, respectively (g/L for both). Our hypothesis is that underlying characteristics of biomarker trajectories may support treatment choice. Baseline covariates collected at initial diagnosis are also available, such as sex, ethnicity, Eastern Cooperative Oncology Group (ECOG), and International Staging System (ISS), age, albumin, beta-2-microglobulin (B2M), creatinine, hemoglobin, lactate dehydrogenase (LDH), lymphocyte count, neutrophil count, platelet count, immunoglobulin A (IgA), immunoglobulin G (IgG), immunoglobulin M (IgM). Furthermore, we also considered the duration of RVd treatment in the first line of therapy as a covariate. Descriptive summaries for outcomes and baseline covariates can be found in Supplementary Appendix A.

## 2.3 Treatment of continuous baseline covariates

Most continuous covariates contain missing data (10%-56%). In order to address this issue, we apply a log transformation to reduce asymmetry, a standardization (z-score) so that their scales are similar, and a mean imputation to replace missing values. Supplementary Appendix A shows a descriptive summary of these covariates before and after being treated. It is worth mentioning that we also performed the analyses without imputation and, although the sample size was greatly reduced, the conclusions were consistent with those using imputation (see Section 5).

# 3 Joint modeling framework

We propose a new Bayesian joint model of multiple longitudinal and categorical outcomes for MM data presented in Section 2. We adopt the shared-parameter specification (Wu and Carrol, 1988), where the longitudinal and categorical processes depend on a hidden process defined by random effects. Below we present the submodels and priors that make up the proposed joint model.

## 3.1 Longitudinal submodels

To describe the patient-level time evolution of M-spike ( $k = 1$ ) and FLC ( $k = 2$ ) biomarkers, we consider a bi-exponential model (Stein et al., 2008), which has already been successfully applied in an MM framework

(Alvares et al., 2025) and is described as follows:

$$y_{ki}(t) = B_{ki} \left[ \exp \{G_{ki}t\} + \exp \{-D_{ki}t\} - 1 \right] + \epsilon_{ki}(t), \quad (1)$$

where  $y_{ki}(t)$  is the  $k$ th biomarker for patient  $i = 1, \dots, n$  at time  $t$ ;  $B_{ki} = \exp \{\theta_{1k} + b_{1ki}\}$ ,  $G_{ki} = \exp \{\theta_{2k} + b_{2ki}\}$ , and  $D_{ki} = \exp \{\theta_{3k} + b_{3ki}\}$  are underlying characteristics of the longitudinal process and represent base-line, growth rate, and decay rate, respectively, where  $\boldsymbol{\theta}_k = (\theta_{1k}, \theta_{2k}, \theta_{3k})^\top$  are population parameters and  $\mathbf{b}_{ki} = (b_{1ki}, b_{2ki}, b_{3ki})^\top$  are random effects. Such random effects follow a zero-mean multivariate normal distribution with unstructured variance-covariance matrix  $\boldsymbol{\Omega}_k$ . The residual errors,  $\epsilon_{k1}(t), \dots, \epsilon_{kn}(t)$ , are assumed to be independently normally distributed with mean zero and variance  $\sigma_k^2$ .

It is worth noting that we assumed that the M-spike and FLC trajectories are independent. Mathematically, this assumption was made to overcome convergence issues associated with a common unstructured variance-covariance matrix for all random effects. However, in medical practice, these biomarkers are expected to be complementary but not necessarily correlated (Tacchetti et al., 2017; Gran et al., 2021), which is aligned with what we assumed.

### 3.2 Categorical submodel

To model the treatment assigned to each patient in the second line of therapy, we consider a (nominal) categorical model (Agresti, 2013). Specifically, let  $z_i \in \{1, 2, \dots, J = 3\}$  be a treatment indicator for patient  $i = 1, \dots, n$ . Then, assuming a log-odds specification, the categorical submodel for  $z_i$  can be written as

$$z_i \sim \text{Categorical}(J, \phi_i) \quad (2)$$

$$\log \left( \frac{\phi_{ij}}{\phi_{iJ}} \right) = \mathbf{X}_i^\top \boldsymbol{\beta}_j + \sum_{k=1}^2 \left( \alpha_{1kj} B_{ki}^* + \alpha_{2kj} G_{ki}^* + \alpha_{3kj} D_{ki}^* \right),$$

where we contrast each  $j = 1, \dots, J - 1$  with category  $J$ . In our application,  $j = 1$  and  $j = 2$  are Carfilzomib-based and Pomalidomide-based therapies, respectively, and  $J = 3$  represent other therapies (reference). The probability vector  $\phi_i = (\phi_{i1}, \dots, \phi_{iJ})^\top$  is defined on the simplex  $\mathcal{S}^{J-1} = \{\phi_i : \phi_{ij} \geq 0, \sum_{j=1}^J \phi_{ij} = 1\}$ ;  $\mathbf{X}_i$  is the baseline covariate vector with coefficients  $\boldsymbol{\beta}_j$ ;  $B_{ki}^* = \log(B_{ki})$ ,  $G_{ki}^* = \log(G_{ki})$ , and  $D_{ki}^* = \log(D_{ki})$  are the baseline, growth rate, and decay rate (in log scale) of the  $k$ th biomarker for patient  $i$ , shared from the longitudinal submodel (1), where  $\alpha_{1kj}$ ,  $\alpha_{2kj}$ , and  $\alpha_{3kj}$  are the coefficients that measure the association of such characteristics with the chosen treatment.

### 3.3 Prior elicitation

We consider standard priors for parameters associated with biomarkers ( $k = 1, 2$ ) and category outcomes ( $j = 1, 2$ ), but we acknowledge the possibility of using alternative priors. In particular, we assume independent and weakly informative marginal prior distributions. For the bi-exponential submodel (1): population

parameters,  $\theta_{1k}$ ,  $\theta_{2k}$ , and  $\theta_{3k}$ , follow  $\text{Normal}(0, 10^2)$  prior distributions; residual error variance,  $\sigma_k^2$ , follows a half-Cauchy(0, 5) prior distribution; and random effects variance-covariance matrix,  $\mathbf{\Omega}_k$ , follows an inverse-Wishart( $\mathbf{I}_3, 4$ ) prior distribution, which is a minimally informative specification (Schuurman et al., 2016), where  $\mathbf{I}_3$  represents a  $3 \times 3$  identity matrix. For the categorical submodel: regression coefficients,  $\beta_j$ , and association parameters,  $\alpha_{1kj}$ ,  $\alpha_{2kj}$ , and  $\alpha_{3kj}$ , follow  $\text{Normal}(0, 10^2)$  prior distributions. As a sensitivity analysis, we also set  $\text{Normal}(0, 100^2)$  and half-Cauchy(0, 25) prior distributions in order to make them less informative. The results were equivalent in terms of posterior distributions obtained, differing only in computational time, so we concluded that our initial choice is weakly informative and speeds up the processing time to achieve convergence of Markov chains.

### 3.4 Posterior inference

Let  $\Psi_1 = (\text{vec}(\mathbf{\Omega}_1)^\top, \sigma_1^2)^\top$ ,  $\Psi_2 = (\text{vec}(\mathbf{\Omega}_2)^\top, \sigma_2^2)^\top$ , and  $\Phi = (\beta_1^\top, \beta_2^\top, \alpha_{\cdot 11}^\top, \alpha_{\cdot 21}^\top, \alpha_{\cdot 12}^\top, \alpha_{\cdot 22}^\top)^\top$  be parameter vectors of the submodels associated with M-spike, FLC, and treatment outcomes, respectively. Also, let  $\theta_1$ ,  $\theta_2$ ,  $\mathbf{b}_1$ , and  $\mathbf{b}_2$  be the information shared between submodels, where  $\mathbf{b}_k = (\mathbf{b}_{k1}^\top, \dots, \mathbf{b}_{kn}^\top)^\top$  is the vector of all random effects of the  $k$ th biomarker. Denoting  $\mathcal{D} = \{\mathbf{y}_{1i}, \mathbf{y}_{2i}, z_i, \mathbf{X}_i; i = 1, \dots, n\}$  as the observed data, under the shared-parameter assumption, the joint posterior distribution of all parameters and random effects is proportionally expressed as follows:

$$\begin{aligned} \pi(\Psi_1, \Psi_2, \Phi, \theta_1, \theta_2, \mathbf{b}_1, \mathbf{b}_2 \mid \mathcal{D}) \propto & f_1(\mathbf{y}_1 \mid \Psi_1, \theta_1, \mathbf{b}_1) f_2(\mathbf{y}_2 \mid \Psi_2, \theta_2, \mathbf{b}_2) f_3(z \mid \Phi, \theta_1, \theta_2, \mathbf{b}_1, \mathbf{b}_2) \times \\ & \times g_1(\mathbf{b}_1 \mid \Psi_1) g_2(\mathbf{b}_2 \mid \Psi_2) \pi(\Psi_1, \Psi_2, \Phi, \theta_1, \theta_2), \end{aligned} \quad (3)$$

where  $f_1(\cdot)$  and  $f_2(\cdot)$  are Normal density functions derived from (1);  $f_3(\cdot)$  is a probability mass function defined as  $\mathbb{P}(Z_i = j) = \phi_{ij}$  for  $j = 1, 2$ , where  $\phi_{ij}$  is calculated as in (2);  $g_1(\cdot)$  and  $g_2(\cdot)$  are Normal density functions for random effects  $\mathbf{b}_1$  and  $\mathbf{b}_2$ , respectively; and  $\pi(\cdot)$  is the prior distribution specified as in Section 3.3.

## 4 Variable importance

Variable importance (VI) is a widely known tool in machine learning (Casalicchio et al., 2019), but it has not been widely adopted in statistical modeling. The concept of VI is to measure the importance of covariates by their ability to improve the prediction model's accuracy. VI and other interpretability techniques can be divided into two groups: *model-specific* and *model-agnostic*. Model-specific techniques are based on assumptions imposed by a specific model, whereas model-agnostic ones do not rely on a predefined structure and can be applied to various problems/models without need for extensive customization or fine-tuning (Chen et al., 2023). In this work, we focus on the model-agnostic approach due to its versatility and easy adaptation to different contexts (Ribeiro et al., 2016). In particular, we use the permutation-based VI strategy proposed by Fisher et al. (2019).

Taking a baseline performance metric ( $M_{\text{base}}$ ) for the fitted model with all variables  $(x_1, x_2, \dots, x_P)$ , Fisher

et al. (2019) showed that the performance metric degrades when considering a random permutation of variable  $x_p$ , while the rest of the variables remain unchanged. Without loss of generality, assuming that a lower metric performance value is better, the permutation-based importance score for  $x_p$  can be computed as  $VI_p = M_p - M_{\text{base}}$ , with  $M_p$  being the performance metric evaluated on the data where only  $x_p$  is randomly permuted. This process is repeated for the  $p$  variables and then their scores are ranked, where the highest VI score indicates the most important variable. Algorithm 1 summarizes this procedure.

---

**Algorithm 1** Permutation-based variable importance algorithm.

---

- 1: Model fitted with all variables  $x_1, x_2, \dots, x_P$ .
  - 2: Compute the performance metric for the fitted model ( $M_{\text{base}}$ ).
  - 3: **for**  $p = 1, \dots, P$  **do**
  - 4:     Permute the values of  $x_p$ .
  - 5:     Compute the performance metric on the permuted data ( $M_p$ ).
  - 6:     Compute the variable importance:  $VI_p = M_p - M_{\text{base}}$ .
  - 7: **end for**
  - 8: Plot ranked  $VI_1, VI_2, \dots, VI_P$ .
- 

The choice of performance metric is an arbitrary decision and may be conditioned on the type of model analyzed. In this work, we used the widely applicable information criterion (WAIC) (Watanabe, 2010), but the VI ranking was identical when applying the leave-one-out cross-validation (Vehtari et al., 2017). Furthermore, due to randomness, calculating VI more than once might greatly vary the results. This problem is mitigated by repeating Algorithm 1 several times and averaging the VI score of each variable. This strategy also allows us to evaluate the variability of VI scores, for example, by using their minimum and maximum values among the repetitions of the same variable. Finally, it is worth mentioning that after each permutation the model does not require refitting; we only recompute the performance metric.

## 5 MM data analysis

Our Bayesian joint model was implemented in Stan using the **rstan** package version 2.26.23 (Stan Development Team, 2023) from the R language version 4.3.1 (R Core Team, 2023). All codes are publicly available at [www.github.com/daniloalvares/BJM-MBiExp-Categ](https://www.github.com/daniloalvares/BJM-MBiExp-Categ). We set three Markov chains with 4000 posterior samples after 1000 warm-up iterations. Under this configuration, posterior samples achieved convergence (Gelman-Rubin statistic,  $R\text{-hat} < 1.05$ ) and efficiency (effective sample size,  $\text{neff} > 500$ ) (Vehtari et al., 2021).

As a competing model, we propose the categorical model described in (2) without considering the latent characteristics shared from the bi-exponential submodels. This model helps to verify whether our joint model is really needed.

We evaluate the goodness-of-fit of the joint and competing models, considering metrics compatible with the nature of each outcome. For bi-exponential submodels, individual weighted residuals (IWRES) across time by biomarker did not suggest any model misspecification (Desmée et al., 2017), as the points are evenly scattered around the horizontal zero-line (see Supplementary Appendix C). For the categorical submodel and

the competing model, class-weighted classification metrics were applied, such as accuracy, precision, recall, and F1-score (see formulas in Supplementary Appendix B). Table 1 shows the percentage of each metric for both models and using a random classifier.

Table 1: Class-weighted classification metrics from the joint model, only categorical model (no longitudinal information), and a random classifier (average of 1000 runs).

	<b>Accuracy &amp; Recall*</b>	<b>Precision</b>	<b>F1-score</b>
Joint model (1)-(2)	72.13%	75.19%	61.23%
Only categorical model	62.89%	58.06%	60.13%
Random classifier	33.33%	55.47%	38.29%

\*Mathematical equivalence in this particular setting (see Supplementary Appendix B).

The joint model proved to be better than the categorical model in all metrics, with greater and smaller differences for accuracy and F1-score, respectively. This corroborates our hypothesis that underlying characteristics of biomarker trajectories help explain the physician’s chosen treatment. In addition, our proposal was significantly superior to the random classifier in all metrics, demonstrating that the joint model results are satisfactory. Still, it is worth mentioning that the treatment decision is a medical choice that may take into account factors not addressed in this study as well as qualitative aspects of daily clinical practice that are not available. Finally, we also compared both models in terms of WAIC and again the joint model (WAIC=2486) was better than the categorical model (WAIC=2527).

Figure 1 shows the VI ranking for the joint model (1)-(2) based on 50 runs. Note that the minimum and maximum values of VI scores for each variable provide a margin of variation that is useful for evaluating potential importance ties.

We observed a clear higher importance for the top three, growth M-spike, baseline FLC, and decay FLC, where all of them presented VI scores that are considerably higher than the others, with minimal overlap between their margins of variation. This means that, in terms of predictive robustness, the growth rate of the M-spike trajectory, the initial FLC value and its decay rate over time are the characteristics that most impact the predicted treatment for the second line of therapy in a subpopulation initially treated with RVd. Growth FLC, decay M-spike, and age occupy positions from 4 to 6 in the ranking, where when analyzing their margins of variation there is no obvious order between them, but their average scores are higher than the subsequent ranked variables. The average score of the subsequent variables is capable of ranking them, but their margins of variation present non-negligible intersections. Supplementary Appendix D shows the VI ranking using the categorical model (no longitudinal information). Except for the shared latent characteristics, the competing model VI ranking produces results very similar to Figure 1.

Table 2 shows the inferential results in terms of relative risk (exponentialized coefficient) from the categorical submodel considering Carfilzomib vs Other and Pomalidomide vs Other, as well as the VI ranking described in Figure 1.

In Table 2, we highlight ECOG 2<sup>+</sup>, age and RVd duration, which are significant and present relative risks in opposite directions for Carfilzomib and Pomalidomide compared to the reference treatment. For example, for



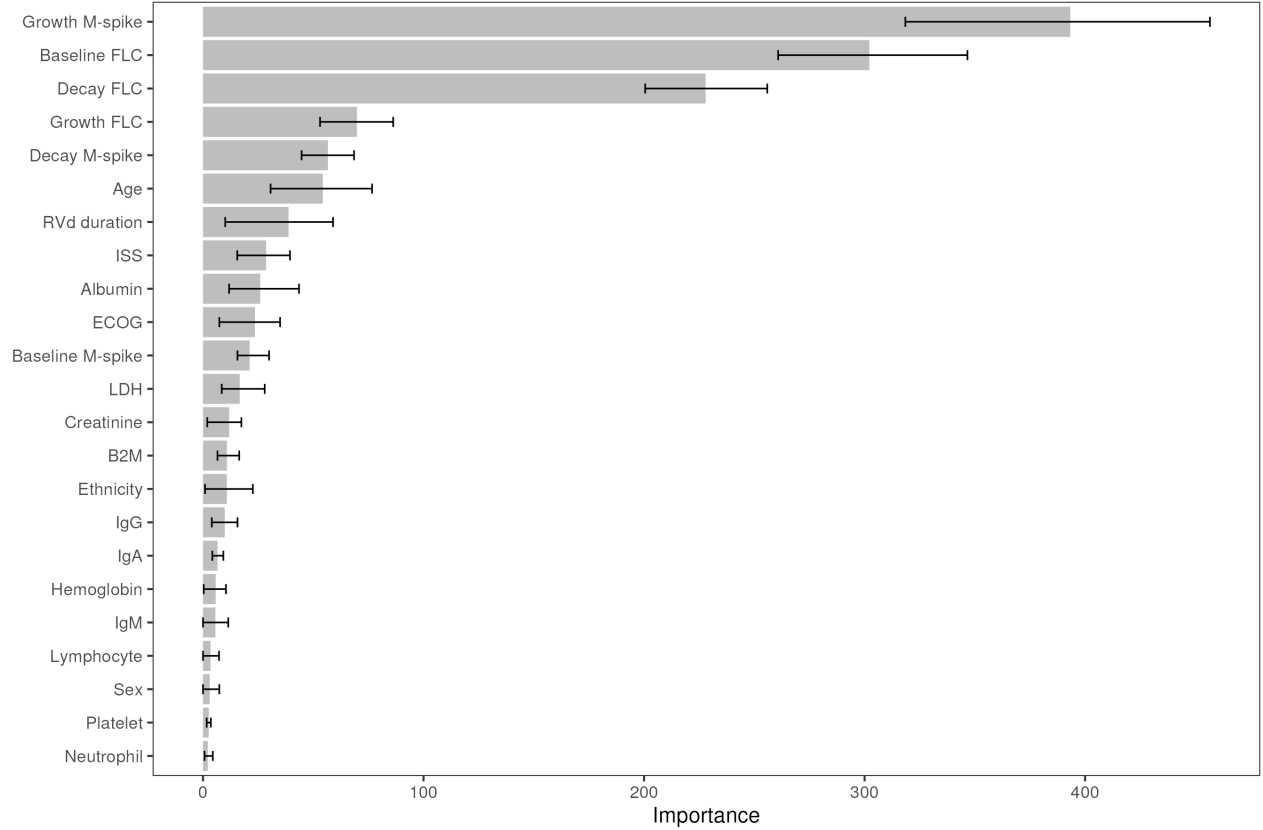


Figure 1: Variable importance (VI) ranking from the joint model (1)-(2). Bar length, lower and upper limits of the horizontal lines represent average, minimum and maximum VI scores, respectively, based on 50 runs.

RVd duration, this means that the relative risk ratio for a one-year increase in RVd treatment time in the first line of therapy is 1.32 ( $1/0.76$ ) for being treated with Other over Carfilzomib, while this ratio is 1.19 in favor of Pomalidomide when contrasted with Other. Conversely, the significant M-spike and FLC characteristics are consistent for both comparisons. Indeed, increasing the M-spike decay rate favors the choice of Other over Carfilzomib or Pomalidomide. On the other hand, starting RVd treatment with a high FLC value or increasing the growth FLC rate throughout the first line of therapy increases the likelihood of choosing Carfilzomib or Pomalidomide over Other for the second line of therapy. Supplementary Appendix D shows that the inferential results using the categorical model (no longitudinal information) are consistent with those in Table 2, except for the M-spike and FLC characteristics that are not present in the competing model.

Clinically, one may also be interested in identifying significant factors between Carfilzomib and Pomalidomide. This analysis can be done by inspecting non-intersecting 95% credible intervals per variable. For example, from Table 2, we can list ECOG  $2^+$ , age, albumin, and RVd duration as significant factors that differentiate the choice between Carfilzomib and Pomalidomide. It is worth noting that latent characteristics of M-spike and FLC trajectories are not statistically relevant when contrasting Carfilzomib and Pomalidomide.

Estimated parameters for the bi-exponential M-spike and FLC submodels are provided in Supplementary Appendix C. Population parameters show similar shapes for the average trajectories of M-spike and FLC

Table 2: Relative risk (RR) and its 95% credible interval (CI) from the categorical submodel parameters for Carfilzomib vs Other and Pomalidomide vs Other, and variable importance (VI) ranking. Statistically significant variables are shown in bold.

Variable	Category	VI ranking	Carfilzomib vs Other RR (95% CI)	Pomalidomide vs Other RR (95% CI)
Sex	Female	21	0.89 (0.68, 1.16)	1.01 (0.75, 1.36)
Ethnicity	Non-Hisp. Black	15	0.96 (0.67, 1.37)	0.74 (0.48, 1.12)
	Other		1.18 (0.84, 1.62)	1.04 (0.73, 1.49)
ECOG	1	10	0.81 (0.57, 1.13)	1.01 (0.68, 1.51)
	2+		<b>0.59</b> (0.37, 0.94)	<b>1.68</b> (1.08, 2.63)
ISS	Stage II	8	1.23 (0.83, 1.82)	0.75 (0.49, 1.13)
	Stage III		1.14 (0.68, 1.92)	1.22 (0.70, 2.10)
Age	–	6	<b>0.76</b> (0.68, 0.86)	<b>1.25</b> (1.07, 1.47)
Albumin	–	9	1.14 (0.96, 1.36)	<b>0.80</b> (0.70, 0.91)
B2M	–	14	1.11 (0.88, 1.39)	0.95 (0.73, 1.23)
Creatine	–	13	1.15 (0.98, 1.34)	0.95 (0.78, 1.14)
Hemoglobin	–	18	0.92 (0.79, 1.07)	1.00 (0.84, 1.18)
LDH	–	12	<b>1.33</b> (1.11, 1.60)	1.05 (0.85, 1.30)
Lymphocyte	–	20	0.96 (0.83, 1.11)	0.91 (0.77, 1.07)
Neutrophil	–	23	1.03 (0.87, 1.22)	1.00 (0.83, 1.21)
Platelet	–	22	0.98 (0.85, 1.15)	0.99 (0.83, 1.19)
IgA	–	17	1.00 (0.80, 1.25)	0.95 (0.75, 1.20)
IgG	–	16	1.12 (0.90, 1.39)	0.97 (0.76, 1.23)
IgM	–	19	0.94 (0.76, 1.14)	0.86 (0.67, 1.07)
RVd duration	–	7	<b>0.76</b> (0.65, 0.89)	<b>1.19</b> (1.03, 1.37)
Baseline M-spike	–	11	1.13 (0.89, 1.44)	1.14 (0.87, 1.49)
Growth M-spike	–	1	1.15 (0.80, 1.64)	<b>1.57</b> (1.03, 2.36)
Decay M-spike	–	5	<b>0.69</b> (0.53, 0.90)	<b>0.72</b> (0.54, 0.96)
Baseline FLC	–	2	<b>1.41</b> (1.10, 1.82)	<b>1.61</b> (1.24, 2.11)
Growth FLC	–	4	<b>1.67</b> (1.21, 2.30)	<b>1.66</b> (1.18, 2.35)
Decay FLC	–	3	0.81 (0.64, 1.04)	<b>0.65</b> (0.51, 0.82)

biomarkers, where M-spike presents an estimated initial value lower than that of FLC, but its growth and decay rates are higher. Residual error and random effects variances indicate greater variability for FLC trajectories. In addition, significant random effects covariances are consistent for both biomarkers, where the random effects for baseline and growth rate are negatively correlated, while baseline and decay rate are positively correlated.

In general, VI ranking and inference are consistent with each other (see Table 2). For example, both support that latent characteristics shared from the bi-exponential submodels are important to explaining treatment choice. Still, it is worth remembering that VI calculates its scores based on a performance metric (in this work, WAIC), so the VI ranking prioritizes the magnitude of the permutation impact on this metric. In other words, VI is not directly based on statistical significance, so it is expected that both criteria complement each other in the task of identifying relevant prognostic factors for choosing treatment.

To illustrate individual-specific interpretations using our joint modeling, we randomly selected two patients,

named A and B, whose baseline covariates and categorical outcomes are presented in Supplementary Appendix C. Figure 2a shows the M-spike and FLC dynamics of patient A, the fit of these trajectories using bi-exponential submodels, and the predicted probability of each treatment option. Initial M-spike was estimated to be close to 25 g/L with a slight decay over the first year followed by an increase until reaching 30 g/L, while FLC presented values below 20 g/L that were well estimated, but with a beginning of trajectory with great uncertainty due to the absence of FLC measurements for this patient over 40 days after starting RVd treatment. Thereby, the predicted probabilities from the categorical submodel suggested Pomalidomide (highest posterior mean) as a treatment for the second line of therapy, which coincides with the physician’s chosen treatment.

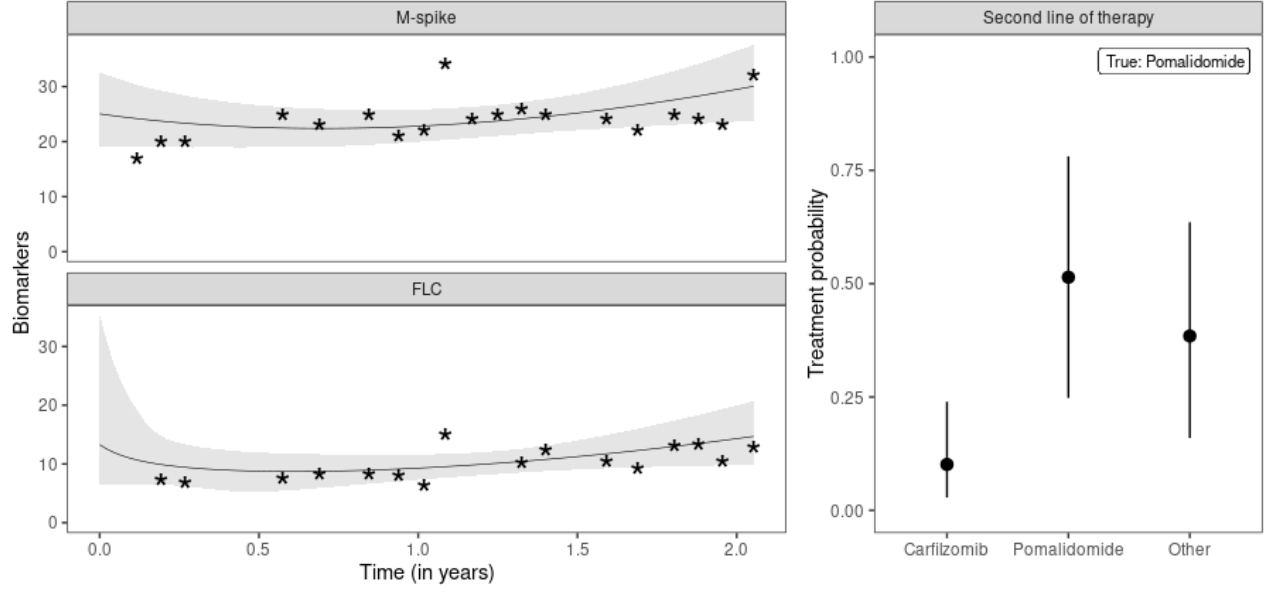
Analogously, Figure 2b shows the estimated trajectories for M-spike and FLC biomarkers of patient B, and the predicted probability of each treatment option for the second line of therapy. Here, the range of longitudinal observations is shorter, but we can notice an M-spike trajectory trend similar to the previous case, but with lower values. On the other hand, the estimated FLC trajectory of patient B is almost constant at 25 g/L, which is clearly higher than that of patient A. This time, the categorical submodel estimated a higher probability for Carfilzomib to be chosen in the second line of therapy, which was also the physician’s selected treatment.

## 6 Discussion

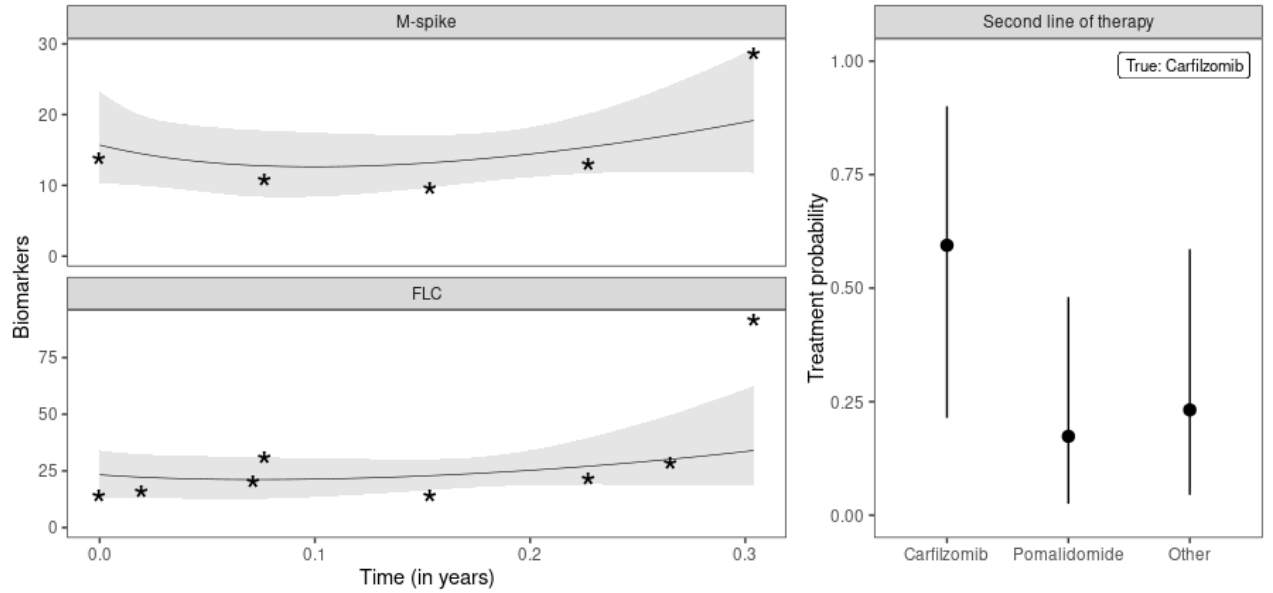
Motivated by a clinical study on MM disease, we have proposed the first Bayesian joint model that accommodates multiple nonlinear longitudinal biomarkers and categorical outcomes. In addition, borrowing ideas from the world of machine learning, we have revisited Fisher et al. (2019)’s proposal to rank the importance of variables from the proposed model applied to MM data.

Evaluation of model fit was performed by residual analysis and multiclass classification metrics. IWRES showed good suitability of the bi-exponential submodel to fit the longitudinal trajectories of M-spike and FLC biomarkers, similar to the results obtained by Alvares et al. (2025). The classification metrics also proved to be satisfactory for a three-class problem, mainly when contrasted with the competing model and a random classifier (see Table 1). VI ranking and inference were concise in pointing out the latent characteristics of biomarker trajectories as relevant prognostic factors for choosing treatment. However, it is also important to remember that VI is based on a predictive performance metric, so some differences between the VI ranking and the inferential significance are expected. Still, VI provides useful and complementary information to the effect sizes, e.g., it proposes a clear ranking of the contribution of each variable to the treatment decision. It should be mentioned that the treatment decision is a medical choice that may take into account relevant clinical parameters not available in this study, such as comorbidities, fitness, treatment toxicity, patient preference, among others. Finally, we illustrated the use of our joint model for two random patients, showing the longitudinal fit of their biomarkers, and their predicted probabilities for each treatment option.

In conclusion, our study has filled a gap in the modeling literature, shed light on topics related to the clinical practice of MM patients, and connected a popular machine learning strategy to a joint model. In future



(a) Patient A.



(b) Patient B.

Figure 2: Left side: observed values (asterisks), posterior mean trajectory (solid line), and 95% credible interval (gray shadow) for each biomarker of patients A and B. Right side: posterior mean (point) and 95% credible interval (vertical line) for each treatment option in the second line of therapy.

work, we envision several extensions of the proposed model. For example, in a high-dimensional longitudinal biomarker framework, the robustness to identify significant association parameters is reduced due to potentially strong correlations among biomarkers, but this problem can be overcome using regularization techniques (Andrinopoulou and Rizopoulos, 2016; Sun and Basu, 2024). We chose a VI strategy as a method for ranking the variables, but the Bayesian framework also provides us with spike-and-slab priors as an alternative approach (Islam et al., 2024). In the presence of heterogeneous subgroups, we recommend adapting our proposal to joint

latent class models (Proust-Lima et al., 2014; Andrinopoulou et al., 2020). In some scenarios, researchers may be interested in studying the causal effect of treatment choice, which requires a causal inference approach (Rizopoulos et al., 2024). Furthermore, the probability for each treatment can be dynamically updated as new longitudinal patient information becomes available (Rizopoulos, 2011; Andrinopoulou et al., 2017). Finally, machine learning algorithms can be proposed for each submodel, such as ensembling techniques for longitudinal data (Hu and Szymczak, 2023) and boosting methods for multiclass classification (Tanha et al., 2020).

## Data availability statement

For eligible studies qualified researchers may request access to individual patient-level clinical data through a data request platform. For up-to-date details on Roche’s Global Policy on the Sharing of Clinical Information and how to request access to related clinical study documents, see the website ([https://go.roche.com/data\\_sharing](https://go.roche.com/data_sharing)). Anonymised records for individual patients across more than one data source external to Roche cannot, and should not, be linked due to a potential increase in risk of patient re-identification. The data that support the findings of this study were originated by and are the property of Flatiron Health, Inc., which has restrictions prohibiting the authors from making the data set publicly available. Requests for data sharing by license or by permission for the specific purpose of replicating results in this manuscript can be submitted to [PublicationsDataAccess@flatiron.com](mailto:PublicationsDataAccess@flatiron.com). The data are subject to a license agreement with Flatiron Health to protect patient privacy and ensure compliance with measures necessary to reduce the risk of re-identification. For example, the data necessary to replicate the study include numerous specific dates, including visit dates (i.e., laboratory or examination dates), treatment start and stop dates, and month of death, as well as laboratory test results. Other measures to maintain de-identification without contractual agreements in place are not feasible due to the study question, methods used, and data elements required.

## Acknowledgements

D.A. and J.K.B. were supported by the U.K. Medical Research Council grant MC.UU.00002/5 and the collaboration grant jointly funded by Roche and the University of Cambridge. The authors thank the following colleagues for helpful discussions during the research and review stage of this work: Vallari Shah, Mellissa Williamson, Sarwar Mozumder, Madlaina Breuleux, Pascal Chanu, and Chris Harbron. For the purpose of open access, the author has applied a Creative Commons Attribution (CC BY) license to any Author Accepted Manuscript version arising from this submission.

## References

Agresti, A. (2013). *Categorical data analysis*. John Wiley & Sons, New Jersey, US, 3rd edition.

- Alsefri, M., Sudell, M., García-Fiñana, M., and Kolamunnage-Dona, R. (2020). Bayesian joint modelling of longitudinal and time to event data: A methodological review. *BMC Medical Research Methodology* **20**, 1–17.
- Alvares, D., Barrett, J. K., Mercier, F., Roumpanis, S., Yiu, S., Castro, F. Schulze, J., and Zhu, Y. (2025). A Bayesian joint model of multiple nonlinear longitudinal and competing risks outcomes for dynamic prediction in multiple myeloma: Joint estimation and corrected two-stage approaches. *Statistics in Medicine* **44**, 1–13.
- Alvares, D. and Rubio, F. J. (2021). A tractable Bayesian joint model for longitudinal and survival data. *Statistics in Medicine* **40**, 4213–4229.
- Andrinopoulou, E. R., Nasserinejad, K., Szczesniak, R., and Rizopoulos, D. (2020). Integrating latent classes in the Bayesian shared parameter joint model of longitudinal and survival outcomes. *Statistical Methods in Medical Research* **29**, 3294–3307.
- Andrinopoulou, E. R. and Rizopoulos, D. (2016). Bayesian shrinkage approach for a joint model of longitudinal and survival outcomes assuming different association structures. *Statistics in Medicine* **35**, 4813–4823.
- Andrinopoulou, E. R., Rizopoulos, D., Takkenberg, J. J. M., and Lesaffre, E. (2017). Combined dynamic predictions using joint models of two longitudinal outcomes and competing risk data. *Statistical Methods in Medical Research* **26**, 1787–1801.
- Birnbaum, B., Nussbaum, N., Seidl-Rathkopf, K., Agrawal, M., Estevez, M., Estola, E., Haimson, J., He, L., Larson, P., and Richardson, P. (2020). Model-assisted cohort selection with bias analysis for generating large-scale cohorts from the EHR for oncology research. *arXiv:2001.09765*.
- Casalicchio, G., Molnar, C., and Bischl, B. (2019). Visualizing the feature importance for black box models. In *Machine learning and knowledge discovery in databases*, pages 655–670, Cham, Switzerland. Springer International Publishing.
- Chen, Z., Xiao, F., Guo, F., and Yan, J. (2023). Interpretable machine learning for building energy management: A state-of-the-art review. *Advances in Applied Energy* **9**, 1–19.
- Chi, M., Wang, X., Song, H., Peng, Y., and Tu, D. (2024). Joint analysis of longitudinal ordinal categorical item response data and survival times with cure fraction. *Statistics in Biopharmaceutical Research* pages 1–11.
- Cho, S., Psioda, M. A., and Ibrahim, J. G. (2024). Bayesian joint modeling of multivariate longitudinal and survival outcomes using Gaussian copulas. *Biostatistics* pages 1–16.
- Choi, J., Cai, J., Zeng, D., and Olshan, A. F. (2015). Joint analysis of survival time and longitudinal categorical outcomes. *Statistics in Biosciences* **7**, 19–47.

- Claret, L., Girard, P., Hoff, P. M., van Cutsem, E., Zuideveld, K. P., Jorga, K., Fagerberg, J., and Bruno, R. (2009). Model-based prediction of phase III overall survival in colorectal cancer on the basis of phase II tumor dynamics. *Journal of Clinical Oncology* **27**, 4103–4108.
- Delporte, M., Molenberghs, G., Fieuws, S., and Verbeke, G. (2024). A joint normal-ordinal (probit) model for ordinal and continuous longitudinal data. *Biostatistics* pages 1–13.
- Desmée, S., Mentré, F., Veyrat-Follet, C., Sébastien, B., and Guedj, J. (2017). Using the SAEM algorithm for mechanistic joint models characterizing the relationship between nonlinear PSA kinetics and survival in prostate cancer patients. *Biometrics* **73**, 305–312.
- Donders, A. R. T., van der Heijden, G. J. M. G., Stijnen, T., and Moons, K. G. M. (2006). Review: A gentle introduction to imputation of missing values. *Journal of Clinical Epidemiology* **59**, 1087–1091.
- Fisher, A., Rudin, C., and Dominici, F. (2019). All models are wrong, but *many* are useful: Learning a variable’s importance by studying an entire class of prediction models simultaneously. *Journal of Machine Learning Research* **20**, 1–81.
- Ganjali, M. and Baghfalaki, T. (2015). A copula approach to joint modeling of longitudinal measurements and survival times using Monte Carlo Expectation-Maximization with application to AIDS studies. *Journal of Biopharmaceutical Statistics* **25**, 1077–1099.
- Gran, C., Afram, G., Liwing, J., Verhoek, A., and Nahi, H. (2021). Involved free light chain: An early independent predictor of response and progression in multiple myeloma. *Leukemia & Lymphoma* **62**, 2227–2234.
- Grandini, M., Bagli, E., and Visani, G. (2020). Metrics for multi-class classification: An overview. *arXiv:2008.05756*.
- Gulla, A. and Anderson, K. C. (2020). Multiple myeloma: The (r)evolution of current therapy and a glance into future. *Haematologica* **105**, 2358–2367.
- Hickey, G. L., Philipson, P., Jorgensen, A., and Kolamunnage-Dona, R. (2016). Joint modelling of time-to-event and multivariate longitudinal outcomes: Recent developments and issues. *BMC Medical Research Methodology* **16**, 1–15.
- Horrocks, J. and van Den Heuvel, M. J. (2009). Prediction of pregnancy: A joint model for longitudinal and binary data. *Bayesian Analysis* **4**, 523–538.
- Hu, J. and Szymczak, S. (2023). A review on longitudinal data analysis with random forest. *Briefings in Bioinformatics* **24**, 1–11.
- Ibrahim, J. G., Chu, H., and Chen, L. M. (2010). Basic concepts and methods for joint models of longitudinal and survival data. *Journal of Clinical Oncology* **28**, 2796–2801.

- Islam, M., Daniels, M. J., Aghabazaz, Z., and Siddique, J. (2024). Bayesian feature selection in joint models with application to a cardiovascular disease cohort study. *arXiv:2412.00885* .
- Keroui, M., Bertrand, J., Bruno, R., Mercier, F., Guedj, J., and Desmée, S. (2022). Modelling the association between biomarkers and clinical outcome: An introduction to nonlinear joint models. *British Journal of Clinical Pharmacology* **88**, 1452–1463.
- Kolo, B. (2010). *Binary and multiclass classification*. Weatherford Press, Weatherford, OK, USA, 1st edition.
- Kumar, S. K., Rajkumar, V., Kyle, R. A., van Duin, M., Sonneveld, P., Mateos, M. V., Gay, F., and Anderson, K. C. (2017). Multiple myeloma. *Nature Reviews Disease Primers* **3**, 1–20.
- Lu, X., Huang, Y., and Zhou, R. (2016). Joint analysis of nonlinear heterogeneous longitudinal data and binary outcome: An application to AIDS clinical studies. *Journal of Applied Statistics* **43**, 2713–2728.
- Ma, X., Long, L., Moon, S., Adamson, B. J. S., and Baxi, S. S. (2023). Comparison of population characteristics in real-world clinical oncology databases in the US: Flatiron Health, SEER, and NPCR. *medRxiv:10.1101/2020.03.16.20037143v3* .
- Martins, R., Silva, G. L., and Andreozzi, V. (2016). Bayesian joint modeling of longitudinal and spatial survival AIDS data. *Statistics in Medicine* **35**, 3368–3384.
- Martins, R., Silva, G. L., and Andreozzi, V. (2017). Joint analysis of longitudinal and survival AIDS data with a spatial fraction of long-term survivors: A Bayesian approach. *Biometrical Journal* **59**, 1166–1183.
- Proust-Lima, C., Séne, M., Taylor, J. M. G., and Jacqmin-Gadda, H. (2014). Joint latent class models for longitudinal and time-to-event data: A review. *Statistical Methods in Medical Research* **23**, 74–90.
- Punke, A. P., Waddell, J. A., and Solimando, D. A. (2017). Lenalidomide, Bortezomib, and Dexamethasone (RVD) regimen for multiple myeloma. *Hospital Pharmacy* **52**, 27–32.
- R Core Team (2023). *R: A language and environment for statistical computing*. R Foundation for Statistical Computing, <https://www.R-project.org/>.
- Rajkumar, S. V. and Kumar, S. (2020). Multiple myeloma current treatment algorithms. *Blood Cancer Journal* **10**, 1–10.
- Rappl, A., Kneib, T., Lang, S., and Bergherr, E. (2023). Spatial joint models through Bayesian structured piecewise additive joint modelling for longitudinal and time-to-event data. *Statistics and Computing* **33**, 1–16.
- Ribeiro, M. T., Singh, S., and Guestrin, C. (2016). Model-agnostic interpretability of machine learning. *arXiv:1606.05386* .



- Rizopoulos, D. (2011). Dynamic predictions and prospective accuracy in joint models for longitudinal and time-to-event data. *Biometrics* **67**, 819–829.
- Rizopoulos, D. (2012). *Joint models for longitudinal and time-to-event data: With applications in R*. Chapman & Hall/CRC, Boca Raton, FL, USA, 1st edition.
- Rizopoulos, D., Taylor, J. M. G., Papageorgiou, G., and Morgan, T. M. (2024). Using joint models for longitudinal and time-to-event data to investigate the causal effect of salvage therapy after prostatectomy. *Statistical Methods in Medical Research* **33**, 894–908.
- Rué, M., Andrinopoulou, E. R., Alvares, D., Armero, C., Forte, A., and Blanch, L. (2017). Bayesian joint modeling of bivariate longitudinal and competing risks data: An application to study patient-ventilator asynchronies in critical care patients. *Biometrical Journal* **59**, 1184–1203.
- Rustand, D., van Niekerk, J., Krainski, E. T., Rue, H., and Proust-Lima, C. (2024). Fast and flexible inference for jointmodels of multivariate longitudinal and survival data using integrated nested Laplace approximations. *Biostatistics* **25**, 429–448.
- Schuurman, N. K., Grasman, R. P. P. P., and Hamaker, E. L. (2016). A comparison of inverse-Wishart prior specifications for covariance matrices in multilevel autoregressive models. *Multivariate Behavioral Research* **51**, 185–206.
- Stan Development Team (2023). *RStan: The R interface to Stan*. Stan, <http://mc-stan.org/>.
- Stein, W. D., Figg, W. D., Dahut, W., Stein, A. D., Hoshen, M. B., Price, D., Bates, S. E., and Fojo, T. (2008). Tumor growth rates derived from data for patients in a clinical trial correlate strongly with patient survival: A novel strategy for evaluation of clinical trial data. *The Oncologist* **13**, 1046–1054.
- Sun, J. and Basu, S. (2024). Penalized joint models of high-dimensional longitudinal biomarkers and a survival outcome. *The Annals of Applied Statistics* **18**, 1490–1505.
- Tacchetti, P., Pezzi, A., Zamagni, E., Pantani, L., Rocchi, S., Zannetti, B. A., Mancuso, K., Ilaria Rizzello, I., and Cavo, M. (2017). Role of serum free light chain assay in the detection of early relapse and prediction of prognosis after relapse in multiple myeloma patients treated upfront with novel agents. *Haematologica* **102**, 104–107.
- Tanha, J., Abdi, Y., Samadi, N., Razzaghi, N., and Asadpour, M. (2020). Boosting methods for multi-class imbalanced data classification: An experimental review. *Journal of Big Data* **7**, 1–47.
- Thai, H. T., Gaudel, N., Cerou, M., Ayral, G., Fau, J. B., Sebastien, B., van de Velde, H., Semiond, D., and Veyrat-Follet, C. (2022). Joint modelling and simulation of M-protein dynamics and progression-free survival for alternative isatuximab dosing with pomalidomide/dexamethasone. *British Journal of Clinical Pharmacology* **88**, 2052–2064.

- van de Donk, N. W. C. J., Pawlyn, C., and Yong, K. L. (2021). Multiple myeloma. *The Lancet* **397**, 410–427.
- Vehtari, A., Gelman, A., and Gabry, J. (2017). Practical Bayesian model evaluation using leave-one-out cross-validation and WAIC. *Statistics and Computing* **27**, 1413–1432.
- Vehtari, A., Gelman, A., Simpson, D., Carpenter, B., and Bürkner, P. C. (2021). Rank-normalization, folding, and localization: An improved  $\hat{R}$  for assessing convergence of MCMC (with discussion). *Bayesian Analysis* **16**, 667–718.
- Wang, C. Y., Wang, N., and Wang, S. (2000). Regression analysis when covariates are regression parameters of a random effects model for observed longitudinal measurements. *Biometrics* **56**, 487–495.
- Watanabe, S. (2010). Asymptotic equivalence of Bayes cross validation and widely applicable information criterion in singular learning theory. *Journal of Machine Learning Research* **11**, 3571–3594.
- Wu, M. C. and Carrol, R. J. (1988). Estimation and comparison of changes in the presence of informative right censoring by modeling the censoring problem. *Biometrics* **44**, 175–188.
- Zhou, G. C., Song, S., and Szczesniak, R. D. (2023). Multilevel joint model of longitudinal continuous and binary outcomes for hierarchically structured data. *Statistics in Medicine* **42**, 2914–2927.

# SUPPLEMENTARY MATERIAL

## Appendix A. Descriptive summaries for MM data

Web Table 1: The 15 most frequent regimens that make up the Other therapy.

Regimen	Number of cases (%)
Dexamethasone + Lenalidomide	123 (11)
Bortezomib + Dexamethasone + Lenalidomide	123 (11)
Daratumumab + Dexamethasone + Lenalidomide	75 (7)
Carfilzomib + Dexamethasone + Pomalidomide	67 (6)
Lenalidomide	56 (5)
Bortezomib + Dexamethasone	54 (5)
Bortezomib + Daratumumab + Dexamethasone	52 (5)
Dexamethasone + Ixazomib + Lenalidomide	51 (5)
Bortezomib + Cyclophosphamide + Dexamethasone	47 (4)
Dexamethasone	39 (3)
Bortezomib	28 (2)
Clinical Study Drug	28 (2)
Daratumumab + Dexamethasone	28 (2)
Bortezomib + Lenalidomide	24 (2)
Bortezomib + Daratumumab + Dexamethasone + Lenalidomide	24 (2)

Web Table 2: Summary of the distribution of the number of M-spike and FLC measurements per patient.

Summary	M-spike	FLC
Min	1	1
Quartile 1	2	3
Median	4	5
Quartile 3	6	8
Max	97	72

Web Table 3: Summary of categorical outcomes and covariates.

Variable	Number of cases (%)
Treatment (outcome)	
Carfilzomib	253 (16)
Pomalidomide	194 (12)
Other	1132 (72)
Sex	
Male	861 (55)
Female	718 (45)
Ethnicity	
Non-Hispanic white	913 (58)
Non-Hispanic black	246 (16)
Other	291 (18)
Not reported	129 (8)
ECOG (Eastern Cooperative Oncology Group)	
0	402 (25)
1	416 (26)
2+	199 (13)
Not reported	562 (36)
ISS (International Staging System)	
Stage I	395 (25)
Stage II	377 (24)
Stage III	326 (21)
Not reported	481 (30)

Web Table 4: Summary of continuous variables in their original scales (Initial) and after log transformation<sup>1</sup>, standardization (z-score), and imputation<sup>2</sup> (Final). NA represents the number of missing observations before imputation.

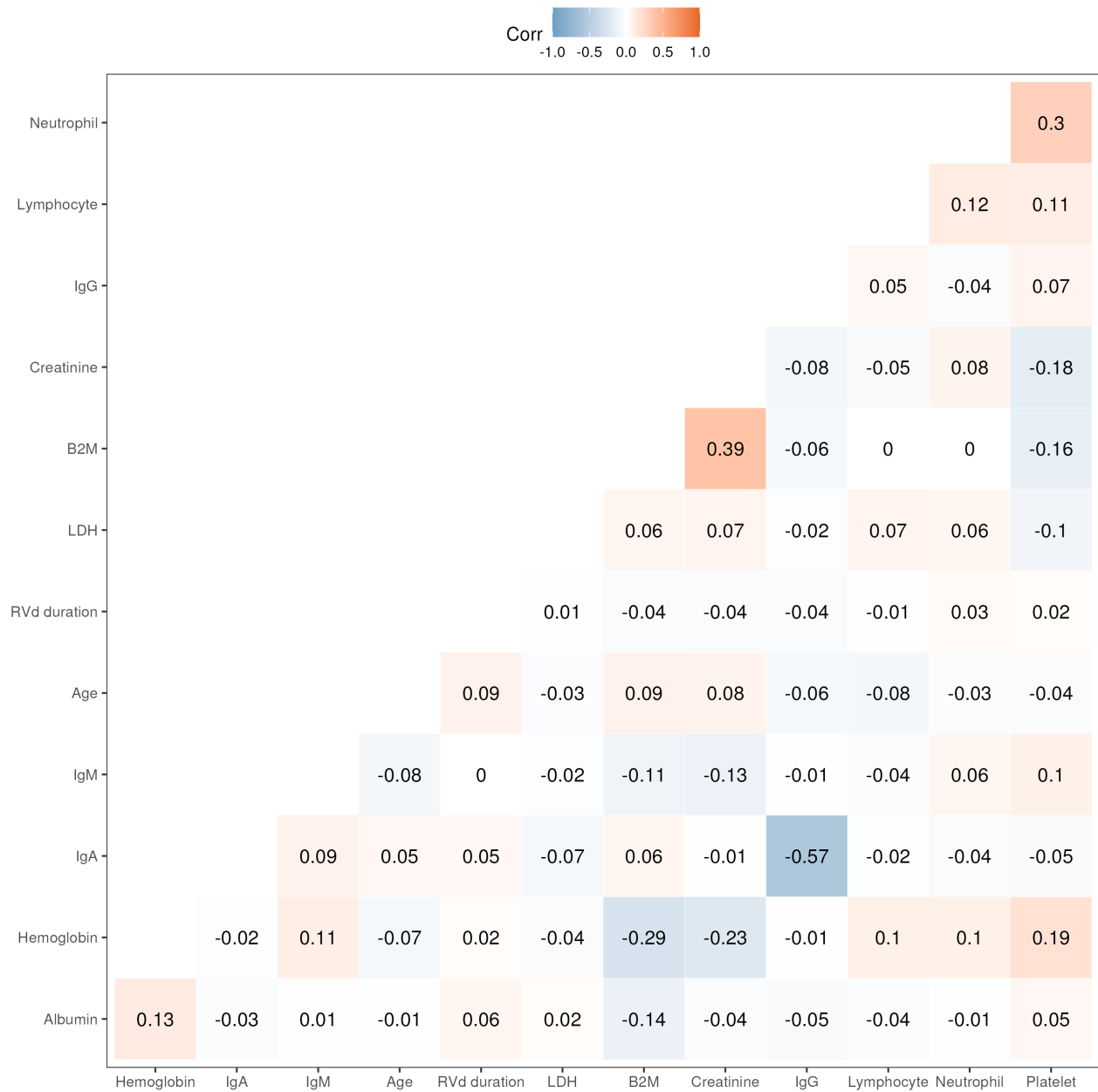
Variable	Data	Mean	SD <sup>3</sup>	Median	Min	Max	NA (%)
Age <sup>4</sup> (years)	Initial	65.29	10.26	67.00	30.00	84.00	–
	Final	0.00	1.00	0.23	-4.47	1.55	–
Albumin (serum, g/L)	Initial	36.73	9.79	38.00	1.00	201.00	371 (23)
	Final	0.00	0.87	0.04	-7.43	3.80	–
B2M (beta-2-microglobulin) (serum, mg/L)	Initial	7.67	71.22	3.85	0.20	2000.00	790 (50)
	Final	0.00	0.71	0.00	-4.04	9.43	–
Creatinine (serum, mg/dL)	Initial	1.29	0.94	1.04	0.40	10.70	373 (24)
	Final	0.00	0.87	0.00	-2.10	5.03	–
Hemoglobin (g/dL)	Initial	10.83	2.20	10.80	4.30	17.70	157 (10)
	Final	0.00	0.95	0.00	-4.28	2.45	–
LDH (lactate dehydrogenase) (serum, U/L)	Initial	224.25	170.17	175.00	50.00	2377.00	891 (56)
	Final	0.00	0.66	0.00	-2.61	4.90	–
Lymphocyte (count, $\times 10^9$ /L)	Initial	1.88	1.31	1.65	0.19	21.33	386 (24)
	Final	0.00	0.87	0.00	-3.73	5.21	–
Neutrophil (count, $\times 10^9$ /L)	Initial	3.87	2.35	3.40	0.41	29.30	582 (37)
	Final	0.00	0.79	0.00	-3.57	4.01	–
Platelet (count, $\times 10^9$ /L)	Initial	227.08	89.61	218.00	29.00	834.00	412 (26)
	Final	0.00	0.86	0.00	-4.88	3.40	–
IgA (immunoglobulin A) (serum, g/L)	Initial	8.09	16.46	0.54	0.00	136.00	717 (45)
	Final	0.00	0.74	0.00	-1.41	2.55	–
IgG (immunoglobulin G) (serum, g/L)	Initial	27.16	26.58	17.05	0.40	139.01	677 (43)
	Final	0.00	0.76	0.00	-2.88	1.88	–
IgM (immunoglobulin M) (serum, g/L)	Initial	0.60	4.55	0.22	0.00	97.43	857 (54)
	Final	0.00	0.68	0.00	-1.84	8.59	–
RVd duration (years)	Initial	1.11	0.97	0.79	0.08	5.82	–

<sup>1</sup>  $\log(x + 0.1)$  to avoid numerical problems when  $x = 0$ .

<sup>2</sup> Mean-value imputation strategy for missing values (Donders et al., 2006), i.e., we replace them with zeros (after standardization, the mean of each variable is zero).

<sup>3</sup> After standardization, the standard deviation is equal to 1, but the imputation concentrates more values at zero and consequently reduces such standard deviation.

<sup>4</sup> Patients with a BirthYear of [Data Cutoff Year - 85] or earlier may have an adjusted BirthYear in Flatiron Health databases due to patient de-identification requirements.



Web Figure 1: Correlation of continuous covariates after log transformation, standardization, and imputation.

## Appendix B. Goodness-of-fit criteria

Individual weighted residuals for longitudinal submodels:

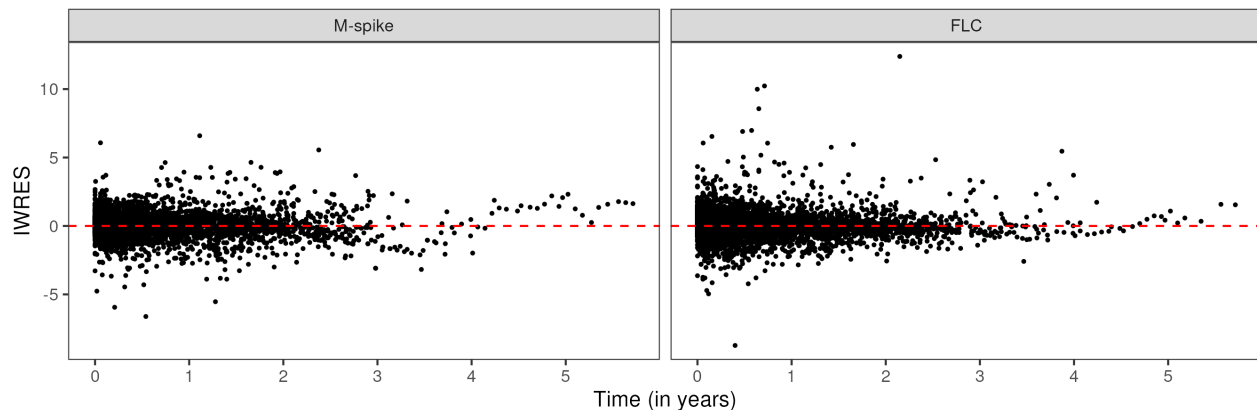
$$\text{IWRES}_i(t) = \frac{y_i(t) - \hat{y}_i(t)}{\hat{\sigma}}$$

Class-weighted classification metrics for categorical submodels:

		Observed			Total
		Treatment 1	Treatment 2	Treatment 3	
Predicted	Treatment 1	TP <sub>1</sub>	·	·	$n_{1(\text{pred})}$
	Treatment 2	·	TP <sub>2</sub>	·	$n_{2(\text{pred})}$
	Treatment 3	·	·	TP <sub>3</sub>	$n_{3(\text{pred})}$
	Total	$n_{1(\text{obs})}$	$n_{2(\text{obs})}$	$n_{3(\text{obs})}$	$N$
Weight		$w_1 = n_{1(\text{obs})}/N$	$w_2 = n_{2(\text{obs})}/N$	$w_3 = n_{3(\text{obs})}/N$	

- Accuracy =  $\frac{1}{N} \sum_{c=1}^3 \text{TP}_c$
- Precision =  $\sum_{c=1}^3 w_c \text{Precision}_c = \sum_{c=1}^3 w_c \left( \frac{\text{TP}_c}{n_{c(\text{pred})}} \right)$
- Recall =  $\sum_{c=1}^3 w_c \text{Recall}_c = \sum_{c=1}^3 w_c \left( \frac{\text{TP}_c}{n_{c(\text{obs})}} \right) = \frac{1}{N} \sum_{c=1}^3 \text{TP}_c = \text{Accuracy}$
- F1-score =  $\sum_{c=1}^3 w_c \left( \frac{2}{\text{Precision}_c^{-1} + \text{Recall}_c^{-1}} \right) = \sum_{c=1}^3 w_c \left( \frac{2}{\frac{n_{c(\text{pred})}}{\text{TP}_c} + \frac{n_{c(\text{obs})}}{\text{TP}_c}} \right)$

## Appendix C. Joint model applied to MM data



Web Figure 2: Individual weighted residuals (IWRES) from the bi-exponential submodel for each biomarker. For suitable fit, IWRES should approximately follow a Normal distribution centered at zero (Keroui et al., 2022).

Web Table 5: Posterior mean and 95% credible interval of the bi-exponential submodel parameters for each biomarker. Statistically significant variables are shown in bold, except for variance parameters.

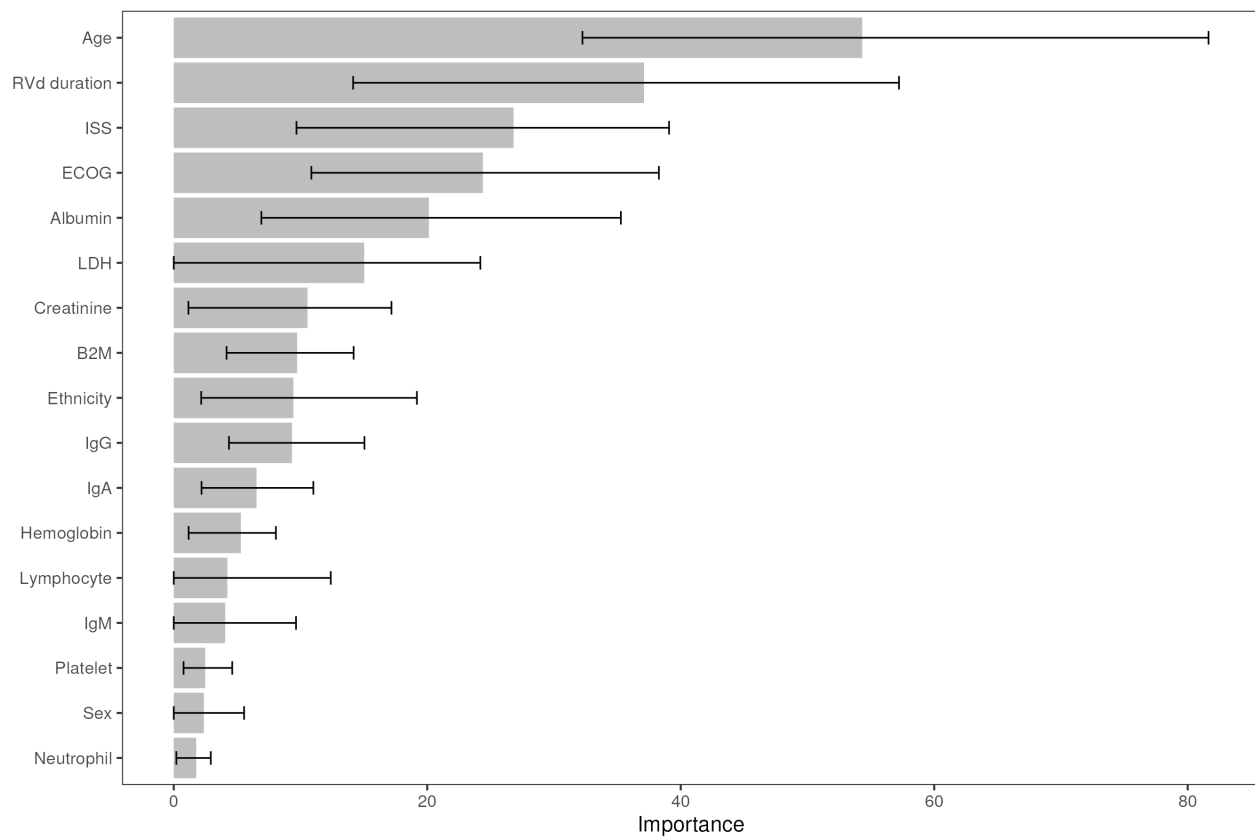
Interpretation	Parameter	M-spike	FLC
Baseline	$\exp\{\theta_{1kl}\}$	<b>18.60</b> (17.62, 19.61)	<b>21.20</b> (19.40, 23.33)
Growth	$\exp\{\theta_{2kl}\}$	<b>0.24</b> (0.22, 0.26)	<b>0.18</b> (0.16, 0.20)
Decay	$\exp\{\theta_{3kl}\}$	<b>4.76</b> (4.42, 5.12)	<b>3.74</b> (3.33, 4.18)
Residual error variance	$\sigma_{kl}^2$	0.06 (0.05, 0.06)	0.14 (0.13, 0.14)
Covariance matrix for random effects	$\omega_{11kl}$	0.79 (0.71, 0.87)	2.93 (2.70, 3.18)
	$\omega_{12kl}$	<b>-0.22</b> (-0.30, -0.15)	<b>-1.37</b> (-1.55, -1.19)
	$\omega_{13kl}$	<b>0.40</b> (0.31, 0.48)	<b>1.62</b> (1.41, 1.85)
	$\omega_{22kl}$	0.70 (0.61, 0.79)	1.60 (1.40, 1.81)
	$\omega_{23kl}$	0.05 (-0.03, 0.13)	-0.04 (-0.22, 0.14)
	$\omega_{33kl}$	0.87 (0.76, 1.00)	2.35 (2.06, 2.66)



Web Table 6: Baseline covariates and categorical outcomes of the illustrative patients.

Variable	Patient A	Patient B
Sex	Information not disclosed for the purpose of anonymization	
Ethnicity		
Age		
ECOG	1	1
ISS	Not reported	Stage III
Albumin (serum, g/L)	33	40
B2B (serum, mg/L)	Not reported	Not reported
Creatinine (serum, mg/dL)	0.7	1.21
Hemoglobin (g/dL)	11.1	7
LDH (serum, U/L)	Not reported	498
Lymphocyte (count, $\times 10^9/L$ )	0.6	0.9
Neutrophil (count, $\times 10^9/L$ )	Not reported	2.6
Platelet (count, $\times 10^9/L$ )	317	69
IgA (serum, g/L)	Not reported	Not reported
IgG (serum, g/L)	Not reported	Not reported
IgM (serum, g/L)	Not reported	Not reported
RVd duration (in years)	2.092	0.326
Physician's chosen treatment (outcome)	Pomalidomide	Carfilzomib

## Appendix D. Competing model applied to MM data



Web Figure 3: Variable importance (VI) ranking from the categorical model (no longitudinal information). Bar length, lower and upper limits of the horizontal lines represent average, minimum and maximum VI scores, respectively, based on 50 runs.

Web Table 7: Relative risk (RR) and its 95% credible interval (CI) from the categorical model parameters (no longitudinal information) for Carfilzomib vs Other and Pomalidomide vs Other, and variable importance (VI) ranking. Statistically significant variables are shown in bold.

Variable	Category	VI ranking	Carfilzomib vs Other RR (95% CI)	Pomalidomide vs Other RR (95% CI)
Sex	Female	16	0.89 (0.69, 1.15)	1.04 (0.79, 1.38)
Ethnicity	Non-Hisp. Black	9	1.04 (0.73, 1.47)	0.81 (0.53, 1.21)
	Other		1.22 (0.89, 1.67)	1.10 (0.78, 1.54)
ECOG	1	4	0.79 (0.57, 1.10)	0.99 (0.68, 1.44)
	2+		<b>0.59</b> (0.37, 0.92)	<b>1.67</b> (1.10, 2.53)
ISS	Stage II	3	1.26 (0.86, 1.84)	0.78 (0.52, 1.17)
	Stage III		1.14 (0.69, 1.88)	1.19 (0.70, 2.02)
Age	–	1	<b>0.77</b> (0.69, 0.86)	<b>1.28</b> (1.10, 1.49)
Albumin	–	5	1.15 (0.98, 1.37)	<b>0.82</b> (0.72, 0.92)
B2M	–	8	1.06 (0.85, 1.32)	0.92 (0.71, 1.19)
Creatine	–	7	1.16 (0.99, 1.35)	0.99 (0.82, 1.18)
Hemoglobin	–	12	0.93 (0.81, 1.08)	1.02 (0.87, 1.19)
LDH	–	6	<b>1.33</b> (1.11, 1.58)	1.06 (0.86, 1.29)
Lymphocyte	–	13	0.95 (0.82, 1.09)	0.89 (0.76, 1.04)
Neutrophil	–	17	1.01 (0.86, 1.19)	0.98 (0.82, 1.17)
Platelet	–	15	0.97 (0.83, 1.13)	0.99 (0.83, 1.17)
IgA	–	11	0.98 (0.80, 1.21)	0.92 (0.74, 1.14)
IgG	–	10	0.95 (0.79, 1.15)	0.95 (0.77, 1.18)
IgM	–	14	0.94 (0.76, 1.14)	0.89 (0.71, 1.10)
RVd duration	–	2	<b>0.76</b> (0.62, 0.84)	1.08 (0.94, 1.23)